4th URSI AT-RASC, Gran Canaria, 19-24 May 2024

Integrating LOFAR and GNSS data for ionospheric perturbation analysis on the January 2022 storm

Rebecca Ghidoni*[1,2], Luca Spogli[2,4], Maaijke Mevius[3], Claudio Cesaroni[2], Lucilla Alfonsi[2], Katarzyna Beser[3,5] and Tiziano Maestri[1]
(1) Alma Mater Studiorum - University of Bologna, Bologna, Italy
(2) Istituto Nazionale di Geofisica e Vulcanologia (INGV), Rome, Italy
(3) ASTRON, Dwingeloo, The Netherlands
(4) SpacEarth Technology, Rome, Italy
(5) Space Research Center, PAS, Warsaw, Poland

Email: rebecca.ghidoni2@unibo.it

Abstract

This study aims at characterizing the multi-scale nature of the processes involved in the dynamic response to the minor geomagnetic storm that occurred on January 14th and 15th, 2022. This is achieved by leveraging the multi-scale reconstruction capabilities enabled through the integration of Low-Frequency Array (LOFAR) and Global Navigation Satellite System (GNSS) measurements in Europe. The LOFAR radio telescope measures intensity across HF-VHF-UHF radio bands emitted by radio-astronomical sources. Simultaneously, GNSS examines ionospheric structures by evaluating the amplitude and phase of L-band signals recorded by ground-based receivers. This combined approach allows for the investigation of ionospheric irregularities with scale sizes ranging from hundreds of meters to a few kilometers.

1.Introduction

The ionosphere, as a dynamic system, demonstrates nonlinear interactions with the various "spheres" that characterize the geospace environment. This nonlinearity is also evident through the diverse range of spatial and temporal scales involved in the ionospheric complex. These different scales play a crucial role in influencing the propagation of trans-ionospheric radio waves. Thus, in recent times, the significance of studying ionospheric disturbances impact on radio communication systems, has been steadily growing. Additionally, the use of the LOFAR radiotelescope data has recently demonstrated to be particularly suited in identifying and studying ionospheric irregularities through scintillation measurements in the HF-VHF-UHF radio bands (see, e.g., [1] and references therein). On the other side, the large number of GNSS receivers offer the possibility to cover large ionospheric sectors and study the ionospheric effects on L-band signals. As a consequence, the wideband spectrum jointly covered by LOFAR and GNSS frequencies allows investigating the energy cascading processes among the various ionospheric spatial scales in unprecedented ways. Between January 14th and 15th, 2022 a G1 geomagnetic storm occurred (Kp max = 6-), triggering ionospheric disturbances on both Earth's hemisphere [2]. The arrival of an Interplanetary Coronal Mass Ejection (ICME) on January 14th caused an increase in the main solar wind parameters resulting into the stormy conditions. Related to this, there was an intensification of the Auroral Electrojet in the European Sector. In particular, Fig. 1 shows the intensification of the electrojet intensity indicator, IE index, crossing the IMAGE magnetometer network of the Finnish Meteorological Institute [3].

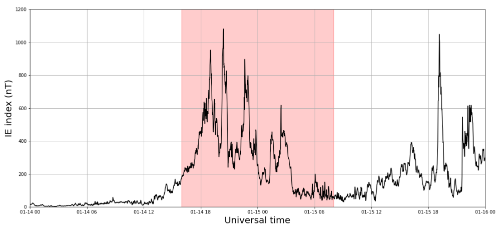

Figure 1. IE index measured by the IMAGE magnetometer network. In red, the variation during the storm. From https://space.fmi.fi/image/www/il_index_panel.php

2. Data and Methods

LOFAR is a large radio telescope network used mainly by astronomers to observe the universe. It is composed by 24 Core stations in Exloo, The Netherlands, by 14 Remote stations in The Netherlands and by 16 International Stations all over Europe.

There are two kinds of antennas: High frequency Band Antennas (HBA) that measure signals at a frequency from 110 to 190 MHz and Low frequency Band Antennas (LBA) that measure a frequency between 10 and 90 MHz [4]. The radio signals arriving at the LOFAR stations are affected by the ionosphere, enabling also its study. On the other hand, GNSS play a crucial role in providing positioning, navigation, and timing information for a wide range of applications, including aviation, maritime navigation, surveying, and location-based services. GNSS receivers serves also as a tool for providing ionospheric information and are widely distributed across the globe. Fig. 2 reports the position of the considered receivers from various GNSS Networks (EUREF, SWEPOS, NMA, NLS, Archivio Dati GNSS Centralizzato" of INGV), in blue, and the International LOFAR stations plus the core station CS002, in red. LOFAR and GNSS are featured by different probing frequencies and observational geometries, that must be carefully considered when the ionospheric effect on those signals must be interpreted. They enable the exploration of diverse scales of ionospheric irregularities, and when studied together, they unveil the multiscale properties of these irregularities.

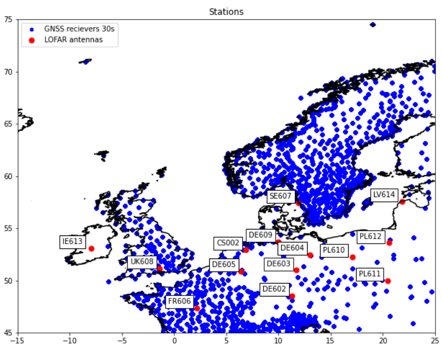

Figure 2. Map of GNSS receivers, in blue, and LOFAR antennas, in red.

Investigated datasets refer to the time window between 16:00 UT on 14 January to 08:00 UT on 15 January (see, also the red box in Fig. 1). We study the variation of the normalized amplitude measured by LOFAR on Cassiopeia A at two different frequency bands of the LBA [around 37 and 57 MHz] at a sampling rate of 1 s. We utilize the amplitude scintillation index S_4, which is defined as the standard deviation of the normalized signal intensity.

$$S_4 = \sqrt{\frac{< I^2 > - < I >^2}{< I >^2}} \quad (1)$$

It is measured over an interval of 60 seconds for every time step. Enhanced values of S_4 indicates the presence of Fresnel's scale irregularities causing diffraction effects [5] on the signal measured by LOFAR.

From GNSS data, we retrieve the Rate of Total Electron Content (TEC) change index ROTI [6]. It is defined as the standard deviation of the rate of TEC (ROT) change over a given time window. ROT is defined as $\frac{dTEC}{dt}$. In this study, ROTI is measured over a time window of 5 minutes, starting from 30 seconds TEC data.

$$ROTI = \sqrt{< ROT^2 > - < ROT >^2} \quad (2)$$

ROTI mostly accounts for the refraction effects of ionosphere on the signal [7].

Despite the fact that these indices assess distinct aspects of the ionospheric perturbation induced on signals, both are affected by irregularities of the order of few tens of kilometers. Ancillary information is provided by the auroral oval reconstruction modeled by leveraging the data from the Special Sensor Ultraviolet Spectrographic Imager (SSUSI) onboard the Defense Meteorological Satellite Program (DMSP) F17 and F18 satellites.

3. Results

Fig. 3 shows the comparison between the time profiles of ROTI, from the GNSS receivers, and of S_4, from LOFAR telescopes at 37 and 55 MHz. The color code represents the value of the latitude of the Ionospheric Pierce Point (IPP) at 350 km. It is worth noticing how the GNSS receivers cover a larger latitudinal range, providing insights of the irregularity forming well within the auroral oval, as further demonstrated below. However, the most interesting feature is the variability of the time profiles in the three different cases. Besides the different latitudinal coverage, this is due to the different probing frequencies and, consequently, to the different scale of the observed irregularities. This further reveal that irregularities of different scale sizes formed during the storm. From now on, we report the LOFAR results only for the 57 MHz frequency, where the higher S_4 values are found, in particular during the ionospheric peak activity of the storm, at 23:10 UT of January 14th. To investigate the ionospheric sectors involved in the formation of the irregularities, we realized geographical maps of ROTI and S_4 for 5 minute intervals. For the sake of brevity, we report in Fig. 4 the map at 23:10 UT of January 14th, which is featured by the largest occurrences of both ROTI and S_4 and that can be, conversely, considered to be the peak of the ionospheric irregularities formation as the response to the geospace forcing. Blue dots show the LOFAR data. The blue shade intensity represents the Fresnel's scale for the LOFAR frequency and observational geometry, that ranges from 12 to 32 km, while the dot dimension is proportional to the S_4 value. The yellow-to-black points, on the other hand, represent ROTI values above 0.1 TECu/min. Values below this threshold are indicated with a smaller grey dot. The red lines represents the edges of the modeled auroral oval, obtained from the closest (in time) imaging data from the DMSP satellites. Both LOFAR and GNSS data are projected at an IPP of 350 km, if outside the Auroral oval, or 120 km, if inside of it. This is because, the peak height of the the particle precipitation causing ionospheric irregularities within the oval is expected to be located at around 120 km, while outside, F-layer irregularities are more likely to occur. The assumption of 120 km as a reasonable value for the height of the irregularity has been verified by using the ionosonde located in Sodankylä, Northern Finland (not shown).

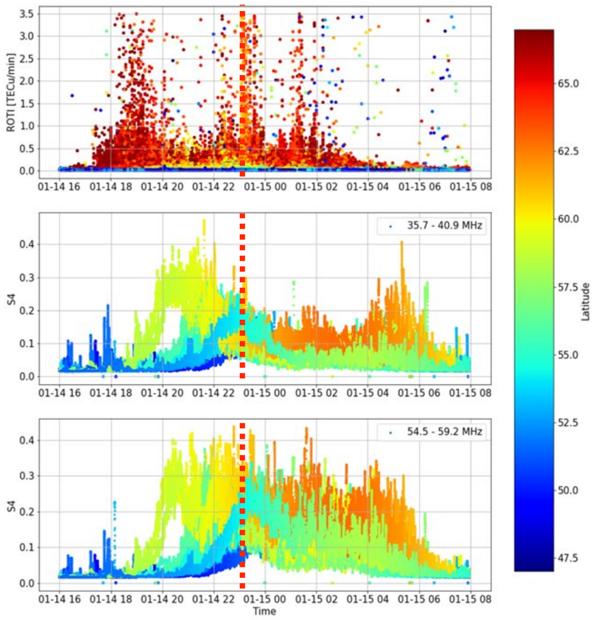

Figure 3. Time profiles of ROTI measured from GNSS signal (upper graph) and S_4 measured by LOFAR (central and lower graphs) during the storm. The color represents the latitude of the signal reported at an IPP of 350 km. The red dotted line corresponds to 23:10 UT of January 14th, the time corresponding to the peak of ionospheric activity induced by the storm.

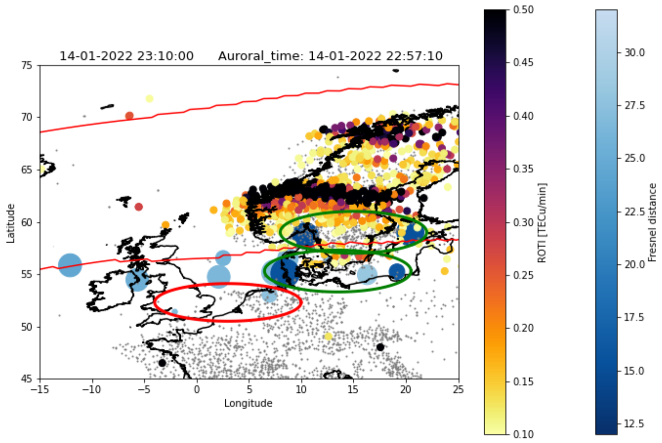

Figure 4. Map of GNSS ROTI and S_4 and Fresnel's scale for LOFAR at 23:10 UT of January 14th. The red lines represent the edges of the auroral oval. The time of DMSP passage is indicated in the plot title. Green and red ovals represent three different ionospheric sectors affected by irregularities.

In Fig. 4, three regions are highlighted by two green ellipses and a red one. The upper green ellipse highlights the increased ROTI and values due to the irregularities formed because of the increased particle precipitation within the auroral oval. The lower green ellipse highlights a region in which S_4 and ROTI enhancements align with the equator-ward edge of the auroral oval. This suggests that these are due to irregularities located to the steep poleward boundary of the ionospheric through, in agreement with [8], which report ROTI values in the range between 0.1 TECu/min and 0.5 TECu/min originating from that. However, the most intriguing region is the red one, signatures of irregularities are captured by LOFAR, but not by GNSS. This is probably due to the scale of the irregularities, that are active for LOFAR S_4 and not effective in raising the GNSS ROTI values.

To investigate the ROTI/S_4 mismatching at sub-auroral, latitudes we extract the time at which the storm reach every international LOFAR stations. Specifically, we investigate the time lag of the peak scintillation occurrence in the considered frequency band as recorded by every LOFAR station with respect to the core station CS002. This lag is reported in Fig.5, which reveals perturbation propagating in the NE-SW direction all over Northern Europe.

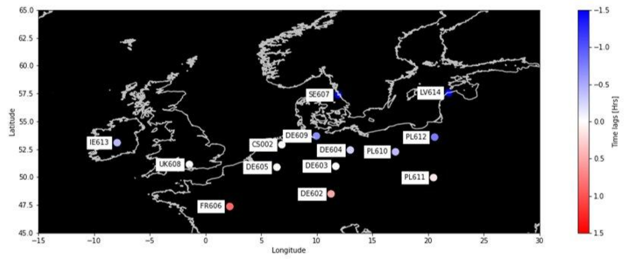

Figure 5. Time lag of the peck scintillation occurrence with respect to CS002. The colors represent the time at which the storm reached every station.

This perturbation has been further confirmed by investigating the spectral power values measured by the Core Stations only in the same period (not shown), revealing then a signature compatible with the presence of Small-scale Traveling Ionospheric Disturbances (SSTIDs), having a wavelength below 30 km. From the core stations, we are able to measure the velocity of this wavelike perturbation according to the following formula:

$$v = \frac{B'T}{||B'T||^2} \qquad (3)$$

in which B is the telescope baseline matrix and T is the delay times matrix. Fig. 6 shows the reconstructed velocities in the NS (blue) and EW (orange) direction during the peak ionospheric activity of the storm. The speed is of the order of some hundreds of m/s, with a slightly higher absolute value for the N/S direction. In Fig 6., the red dashed line indicates the time to which the map reported in Fig. 4 refer. From this, we can have an estimate of the speed of the irregularities involved in the LOFAR scintillation in the sub-auroral region. The velocity of the perturbation is equal to:

$$v_{storm} \approx \sqrt{(350\frac{m}{s})^2 + (700\frac{m}{s})^2} \approx 780\frac{m}{s} \qquad (4)$$

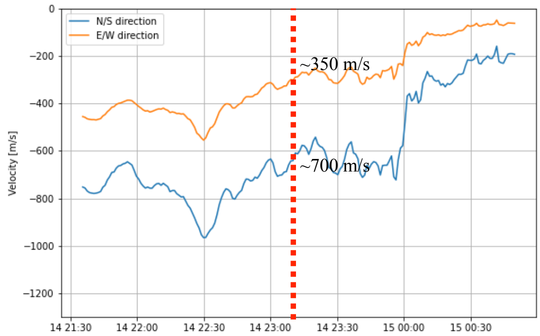

Figure 6. North-South and East-West component of the velocity of the perturbation measured over the LOFAR core stations. The red dotted line correspond to 23:10 UT of January 14th.

We remind the reader that the capability of ROTI to depict specific scales of the irregularities is linked to it sampling rate. Specifically, if the irregularity velocity and the ray path velocity are perpendicular, the scale of the irregularity sampled by ROTI is equal to:

$$r_{irr}^{ROTI} = \frac{v_{irr}}{f_{irr}^{ROTI}} \quad (5)$$

Where f_{irr}^{ROTI} is the Nyquist frequency of the ROTI observation, i.e. $(2 \cdot 30s)^{-1}$ in our case, and v_{irr} is the irregularity speed. As per equation (5), the latter is equal to $780\frac{m}{s} \cdot 60s = 48.6km$, meaning that for GNSS is impossible to measure irregularities caused by Small-Scale TIDs, which have a typical scale size below 30 km, as further confirmed by the Fresnel's scale indicated by the blue shaded Colorbar in Fig. 4. The difference of measurable scale between LOFAR and GNSS is likely the cause of the different perturbations seen by LOFAR and GNSS in the red area in Fig. 4.

4. Conclusions

The joint use of the two instruments reveal the occurrence different kinds of irregularities, affecting LOFAR S_4 and GNSS ROTI, namely the irregularities due to an increase of direct particles precipitation in the auroral oval and the steepening of the edge of the equator-ward ionospheric trough and the one propagating towards lower latitudes likely due to wave-like structures having scale size in the SSTID range. The two instruments are able to measure irregularities of different dimension and so they describe the ionosphere in different ways. This differences are due to the different frequencies, sampling rate and observational geometry of GNSS and LOFAR.
A possibles avenue for future research is analyzing GNSS data at a high rate (1 Hz) promises to enhance scale resolution, allowing insights to be gained on a kilometer-scale level.

5. Acknowledgements

GNSS data are provided by the National Land SurveyFinland NLS (https://www.maanmittauslaitos.fi/en/mapsand- spatial-data/positioning-services/rinex-palvelu), SWEPOS Sweden (https://swepos.lantmateriet.se/), Norwegian Mapping Authority (Kartverket, https://ftp.statkart.no/), and by the "Archivio Dati GNSS Centralizzato" of INGV, which collects GNSS data from eighty networks in the Euro-Mediterranean region and Africa.
This paper is based on data obtained with the International LOFAR Telescope (ILT) under project codes LC7_001 and LC8_001 available through LOFAR Long Term Archive (LTA): https://lta.lofar.eu/Lofar.

References

[1] Flisek P, Forte B, Fallows R, Kotulak K, Krankowski A, et al. 2023. Towards the possibility to combine LOFAR and GNSS measurements to sense ionospheric irregularities. J. Space Weather Space Clim. 13, 27. https://doi.org/10.1051/swsc/2023021

[2] Zhang K and Wang H (2023), Observations and simulations of large-scale traveling ionospheric disturbances during the January 14-15, 2022 geomagnetic storm. Front. Astron. Space Sci. 10:1297632. doi: 10.3389/fspas.2023.1297632

[3] A. Viljanen, L. Häkkinen, IMAGE magnetometer network, in Ground-Based Observations in Support of the Cluster Mission, ed. by M. Lockwood, M.N. Wild, H.J. Opgenoorth. ESA Publications, vol. SP-1198 (ESTEC, Noordwijk, 1997), pp. 111–117

[4] M.P. van Haarlem et al. (2013), LOFAR: The low-frequency array. Astronomy & astrophysics, 556, A2

[5] A. W. Wernik, J. A. Secan, and E. J. Fremouw (2003), Ionospheric irregularities and scintillation, Adv. Space Res., vol. 31, no. 4, pp. 971–981

[6] Pi, X., Mannucci, A. J., Lindqwister, U. J., & Ho, C. M. (1997). Monitoring of global ionospheric irregularities using the worldwide GPS network. Geophysical Research Letters, 24(18), 2283–2286. https://doi.org/10.1029/97gl02273

[7] Spogli, L., Alfonsi, L., and Cesaroni, C. (2023), Stepping Into an Equatorial Plasma Bubble With a Swarm Overfly, Space Weather, vol. 21, no. 5

[8] Cherniak et al. (2015), Dynamics of the high-latitude ionospheric irregularities during the 17 March 2015 St. Patrick's Day storm: Ground-based GPS measurements, Space Weather, 13(9), 585-597.